ACCURACY IMPROVEMENT OF SMALL DEFECT DETECTION FOR ULTRASONIC INSPECTION BY USING SCIENTIFIC VISUAL ANALYSIS

Noboru Sugawara
Department of Civil Engineering
Kitami Institute of Technology
165 Koen-cho, Kitami, Hokkaido, Japan

Toshiyuki Oshima and Shuichi Mikami
Department of Development Engineering
Kitami Institute of Technology

Shinya Sugiura
Konoikegumi Corporation, Tokyo, Japan

INTRODUCTION

When we diagnose the structural integrity of a steel member in service and evaluate its remaining life time, we need to improve analyzing method to get the accurate information of a internal defect of a member. And by the recent demand for high level quality control of welding of steel joint the accuracy improvement of defect detection in the image display became essential in nondestructive evaluation (NDE)[1][2][3]. So far the defect information obtained by an ultrasonic test is displayed in several ways and A-scan and B-scan displays are commonly used in a field inspection and C-scan display is used in laboratory test of the steel structural member[4][5].

In this study we made the different types of artificial small defects by drilled hole in a steel plate specimen to observe by an ultrasonic scanning pulse echo test[6]. The artificial drilled holes with diameter 1mm and 2mm are made with different lengths and inclinations and the graphic images are compared among these cases. 3D images of these defect are obtained by a graphic software[7] on a workstation by using the maximum amplitude data of boundary and bottom echo and time of flight data by which we find from where the incident wave returned back. And in order to apply the C-scope immersion method of ultrasonic test to a field inspection, the effects of surface conditions of specimen are analyzed. The accurate defect size obtained by the ratio of the maximum amplitudes between the boundary echo and bottom echo is shown in the detail waveform analysis of the reflection wave by using Scientific Visual Analysis(SVA).

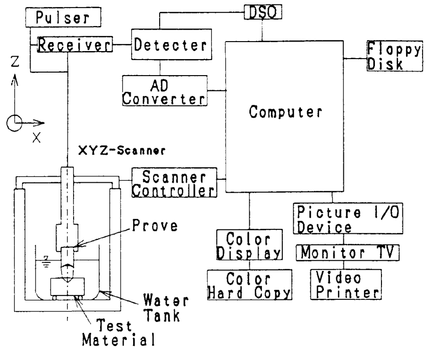

Fig. 1. Measurement system.

Table 1. Specimens.

Type I	ϕ(°)	h (mm)	Type II	ϕ(°)	h (mm)
A	90	5	J	90	5
B		3	K		3
C		2	L		2
D	75	5	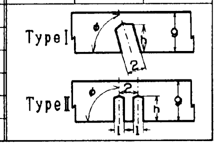		
E		3			
F		2			
G	60	5			
H		3			
I		2			

MEASUREMENT SYSTEM

The measurement system employed in this study is shown in Fig.1. This system of immersion type ultrasonic testing is illustrated by the several parts of subsystem and they are

(1) Image display system
(2) Ultrasonic wave recorder system (Digital storage oscilloscope)
  a) sampling speed 500 Mega samples per second
  b) resolution of amplitude 10 bit
  c) frequency range up to 300MHz

The sampling gate of time axis is set correspond to the thickness of specimen to receive first boundary echo from a defect and bottom echo. Ultrasonic wave recorder system can get the whole reflection waves that passed above mentioned time gate as 4096 data of digital values for every wave and display the spectrum of the detected waves by FFT.

3D DISPLAY OF SMALL DEFECT BY MAXIMUM AMPLITUDE DATA AND TIME OF FLIGHT DATA

Specimen and Measurement

In the steel plate specimen with 9mm thick twelve artificial defects of different types are made by drilled holes as shown in Table 1. Among them there are three types of depth h as 5mm, 3mm, 2mm and three types of inclinations ϕ as 90°,75°,60° of drilled holes, respectively. And the diameters of drilled holes are 2mm and 1mm as shown in Table 1 and two close holes of diameter 1mm at 2 mm distant are used to get the coupling effect of ultrasonic scattering on the image of defect. The kinds of the specimen for coupling effect are named by specimen J,K,L with different depth as 5mm,3mm,2mm as shown in Table 1, respectively. Reflection waves from the defect are measured by using a line scanning along with a distinct line to across the C-scan image of defect. They are discussed later.

Results

By using ultrasonic inspection system we can obtain the maximum amplitude data which represent the distribution of maximum amplitude of echo reflected from the bottom of the plate or boundary of the defect and the time of flight data which represent from where the incident wave returned back. And

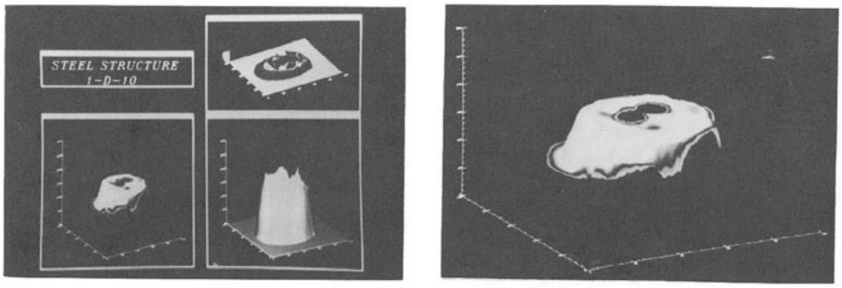

(a) (b)

Fig. 2. D-scan image of specimen D.

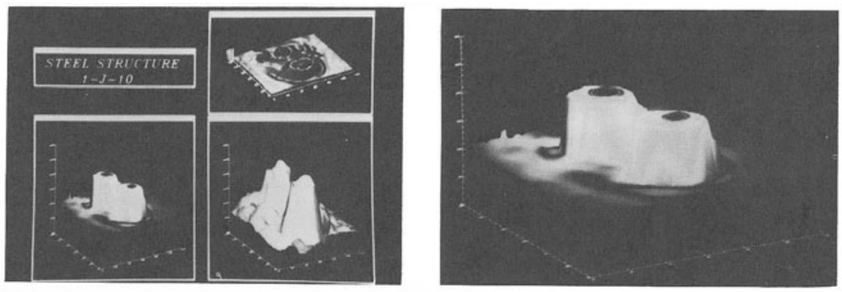

(a) (b)

Fig. 3. D-scan image of specimen J.

with these data we can get the C-scan images of maximum amplitude and time of flight with 256 grades of color display on 2D rectangular coordinate.

In this chapter 3D representation of maximum amplitude data by using a computer graphics (CG) software on a workstation (WS) is shown. The values of 256 color grades which correspond to the amplitude of echo and are on the 2D plane of scanning range, are taken in the vertical coordinate perpendicular to the above 2D plane. And the time of flight data are used like filtering of the boundary echo by which we can pass the boundary echo through to separate from the bottom echo within the scanning range. By this filtering technique we can get the clear 3D images of maximum amplitude data by representing the clear boundary of small defect.

In Fig.2(a) three different 3D images of defect type D as listed in Table 1 are shown. In the lower picture of right hand side in Fig.2(a), the above mentioned 3D representation of the maximum amplitude data by converting the 256 color grades values to the vertical coordinate within the scanning range, is shown by using CG software on the WS display. In the upper picture of right hand side in Fig.2(a) the different representation of the same 3D image is shown by changing the location of view point and the scale of vertical coordinate on CG software. By this picture we can find out the detailed undulation of small defect tip by clear image. In the lower picture of left hand side in Fig.2(a) only the 3D image of a defect shape is shown in the dark background by using the time of flight data to pass only the boundary echo values by a above mentioned filtering technique.

In Fig.2(b) the enlarged picture of the same defect as shown in Fig.2(a) is shown. And by using 3D rotation procedure on CG software we can rotate the 3D image of the defect on the display of WS we can understand the whole shape of a small defect by 3D representation. By these pictures the effect of inclination of drilled holes on the 3D images are clearly obtained. And in Fig.3(a),(b), the 3D image of the defect type J is shown. By using this SVA to obtain a 3D images of small defect we can find out the detailed structure of a defect and thus evaluate the accurate strength of a material. It is called a " D-scope display" of a defect correspond to the A-scope, B-scope and C-scope displays.

APPLICATION OF C-SCAN DISPLAY TO THE FIELD INSPECTION

Effect of Surface Roughness on the C-scan Image Analysis

In order to investigate the effect of surface roughness of the specimen on the accuracy of the defect detection, the grains of sand are spread on the steel plate of 6mm thick and made artificial surface roughness on the upper surface of the specimen. The drilled hole of diameter 4mm and length 3mm is made on the lower surface of the specimen.

The grain sizes of sand are 0.15mm, 0.2mm and 0.3mm for three different specimens, respectively, and the power spectrum of surface roughness in the case of grain size 0.3mm are shown in Fig.4. This result is obtained by the equipment for surface roughness which can scan on the area of artificial defect by 0.1mm pitch. The amplitudes of surface roughness of 101 points over the area of 10mm×10mm(100mm^2) are obtained in this case by 11 lines of equal distance and analyzed by FFT spectrum software. The result shown in Fig.4 is the average power spectrum of surface roughness by the above 11 lines of equal distance over the defect.

The straight line is given by

$$S=a\Omega^{-n} \tag{1}$$

where S=power spectrum of surface roughness
a,n=parameters for surface roughness
Ω=frequency of surface roughness

The defect diameters on the detected images of drilled hole with real diameter 4 mm and necessary gain values of amplifier of the system in the case of grain size of 0.3mm, are shown in Fig.5. The abscissa of this figure is root mean square of surface roughness. The values shown by the mark × and scaled by the ordinate of right hand side correspond to the results of detected diameters of drilled hole. If the surface roughness becomes large, we need to choose the large gain value for amplification of the measurement. However when we use large amplification, we loose SN ratio at the measurement. Thus the necessary gain values chosen to detect by a good defect images depending on the surface roughness exist which are shown by the mark ○ and scaled by the ordinate of left hand side in Fig.5. We can find in Fig.5 that if the surface roughness becomes large, detected sizes of defect images become scattered by large variance and to be detected by larger sizes. And again necessary gain values to be used depending on the condition of surface roughness of the specimen are given in Fig.5.

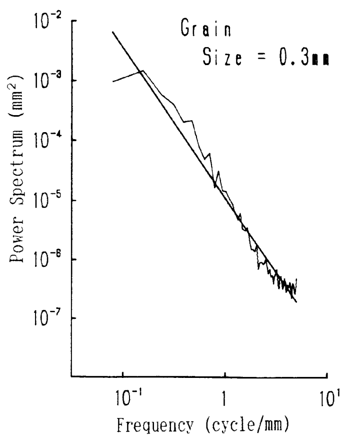

Fig. 4. Power spectrum of surface roughness.

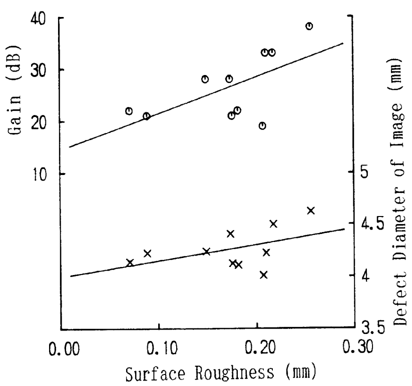

Fig. 5. Effect of sand on steel surface (Grain size is 0.3mm).

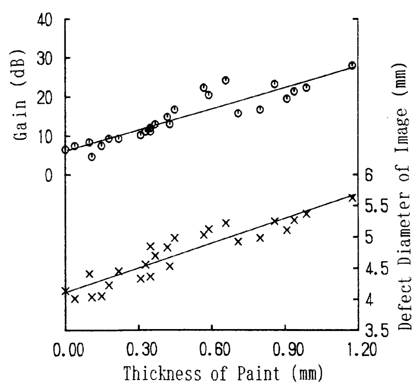

Fig. 6. Effect of paint on steel surface.

Effect of Paint on the Specimen

As a field inspection by C-scan method we have to measure a structural member through the layered paint. If the thickness of paint is thick, because of a damping effect we have to choose a necessary gain to get a accurate image of the defect. The 26 specimens with different thickness of paint and with the drilled holes of same diameter 4mm are used. The defect size of detected images as a function of paint thickness are plotted by the mark × and scaled by the ordinate of right hand side in Fig.6. And if the paint thickness becomes thick, the necessary gain value to get a good image of defect becomes high, and then the defect diameter of detected image becomes larger than the real diameter 4mm as shown in Fig.6.

ACCURATE ANALYSIS OF BOUNDARY ECHO BY SCIENTIFIC VISUAL ANALYSIS

The detected defect image given by ultrasonic scanning test is given by the data of echo amplitude. The echo amplitude data consist of the maximum amplitude of boundary and bottom echo which are reflected from the boundary of a defect and lower surface of the specimen. If the location of probe and the focal point of the incident wave reaches to the boundary of the defect, the boundary echo reflected from the boundary of a defect is detected together with the bottom echo reflected from the lower surface of the specimen within a time gate set up by the system. However we sometimes cannot obtain a good defect image with sufficient accuracy in these measurement because of the wave scattering at the boundary of the defect. This scattering effect on the wave reflection depends upon the wave length and shape and size of a defect. Therefore we need a detail analysis of the boundary echo to get the accurate information on the shape and size of the defect in addition to the C-scan image given by the echo amplitude data.

In this chapter we discuss the precise wave analysis of boundary echo obtained within a time gate set up by the system and find out a method to measure the more accurate size of the defect by using SVA.

Experimental Measurement

The circular drilled holes of diameter 2mm are made in the steel plate of 9mm thick with three different lengths of 5mm, 3mm and 2mm and we call these specimen as specimen A, B and C, respectively. The focus of the probe is first adjusted at the center of drilled hole. And the probe with 10MHz resonance frequency scans over the square of the area of 5mm×5mm on the drilled hole to get the C-scan image of the defect. The reflection waves are received along with the line to across the defect by 50μm pitch around the boundary of the defect and by 100μm pitch for the other area. The reflection waves are transformed to the digital data by using the digital storage oscilloscope(DSO) and stored to a floppy disk. The sampling pitch of time is 0.57nsec and the number of data for the one reflection wave is 4096 points.

At the same time we can get the Fourier spectrum of the wave by a FFT analysis software of DSO on the monitor. In Fig.7 (a),(b) the typical original data received by the ultrasonic scanning test are shown. In Fig.7(a) the transition of the received wave from the bottom echo(wave ①,②) reflected from the lower surface to the boundary echo(wave ④,⑤) reflected from the defect, when the probe gets into the defect, is clearly shown. And in Fig.7(b) another transition of the received waves from the boundary echo to the bottom echo, when the probe gets out across the defect boundary, is also shown.

In these figures the amplitudes of the waves are normalized by the maximum amplitudes of each waves and the abscissas are scaled by microsecond(μs). The numbers shown in Fig.7(a),(b) as ①,②,etc. indicate the location of the probe where the reflection waves are received and they also correspond to the locations shown in Fig.8.

Results Obtained by Scientific Visual Analysis

The reflection wave involves both the boundary echo and the bottom echo, and when the probe comes to be close to the defect boundary the amplitude of boundary echo becomes greater than that of bottom echo. Then there is a boundary of defect somewhere in the transition range. In the defect image analysis by using the maximum amplitude of the reflection wave we receive the greater amplitude of boundary echo within the area of defect as shown in Fig.7(a),(b) from the wave number ⑤ to ⑧. As we can separate the boundary echo from the bottom echo in the reflection wave, we can get each maximum amplitude of both the boundary echo(Bo) and bottom echo(Ba). And the normal maximum amplitude of the bottom echo(Bao) is also obtained far from the defect boundary.

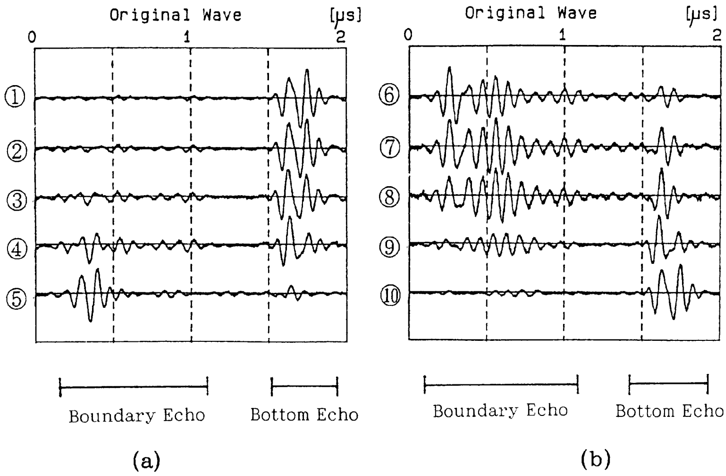

Fig. 7. Measured waveforms of specimen A.

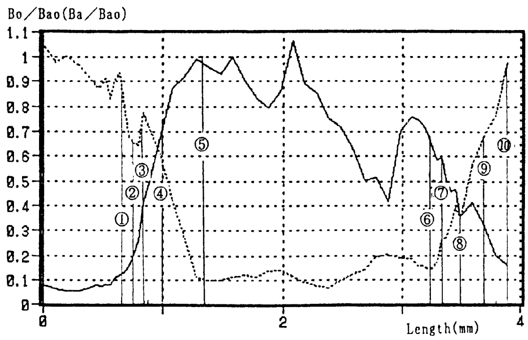

Fig. 8. Results of (Bo/Bao) and (Ba/Bao) for specimen A.

The ratios between the maximum amplitude of the boundary echo (Bo) and the normal maximum amplitude of the bottom echo(Bao) are shown in Fig.8 by the solid lines in the case of specimen A and the ratio between the maximum amplitude of the bottom echo(Ba) and the normal maximum amplitude of the bottom echo (Bao) is also shown by the dotted line. The abscissa is scaled by the distance in millimeter(mm).

We can see in this figure that the ratio of Bo/Bao becomes small within the length nearly equal to 2mm which corresponds to the size of real defect. And the distribution of the ratios of Ba/Bao means the undulation of the drilled hole tip because it corresponds to the distribution of maximum amplitude of boundary echo. The 3D representation of reflection waves are also shown by using SAV in Fig.9 (a) and (b) in the cases of defect A and defect J, respectively. The incident waves come from left hand side. We can see in these pictures that the waves reflect at the defect boundary when the transducer gets into the defect and elsewhere reflect at the bottom of the plate. In these 3D analysis reflection waves of 53 positions of transducer by 50μm pitch are displayed.

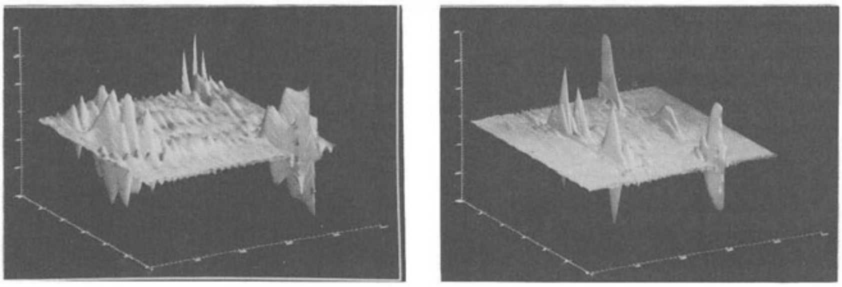

(a) (b)

Fig. 9. 3D representation of reflection waves for specimens A and J.

CONCLUSION

Summarizing the above study on the precise analysis of the reflection wave by using SVA to get a improved image of the defect, we have come to the conclusions as follows;

Twelve C-scan images of small defects are obtained by using ultrasonic scanning system together with the time of flight data which is used to make the defect boundary of image clear. 3D images of small defects are obtained by a CG software on a workstation using both the maximum amplitude data and time of flight data. We call here this 3D image as a D scope image. In order to apply this C-scan measurement of ultrasonic scanning test to the field inspection, the effects of surface roughness and paint thickness of the specimen on the C-scan image of defect are obtained. By using SVA of the reflection wave we can obtain the more accurate defect size given by the distribution of the boundary and bottom echo together with the scattering effect at the defect boundary.

REFERENCES

1. Thompson, D.O. and Chimenti, D.E. : Review of progress in quantitative nondestructive evaluation, Plenum Press, Vol.1(1981)~Vol.10(1991).
2. Miki, C., Fukazawa, M., Katoh, M. and Ohune, H. : Feasibility study on crack detection of fillet welded joint, Proc. of JSCE, No.386, pp329-337, 1987.(in Japanese)
3. Iijima, T., Hukami, M., Miki, C. and Tajima, J.: Study on fatigue crack detection in stiffening truss chord members, Proc. of JSCE, No.410, I-12, pp445-454, 1989.(in Japanese)
4. Krautkr mer, J. and Krautkr mer, H. : Ultrasonic Testing of Materials, Springer-Verlag, 1977.
5. Hull, B. and John, V. : Non-Destructive Testing, Macmillan Education, 1988.
6. Mikami, S., Yamazaki, T., Sugawara, N. and Oshima, T. : Study on the improvement of small defect detection for steel structure by means of ultrasonic pulse echo method, Proc. of The Symposium on Non-Destructive Evaluation in Civil Engineering, JSCE, 1991.(in Japanese)
7. Precision Visuals, Inc. : PV-Wave Overview, 1988.